Egyptian Journal of Veterinary Sciences
https://ejvs.journals.ekb.eg/

The Role of Gold - Silver Nanocomposite Gel versus *Astragalus Polysaccharides* on Healing Process of Experimentally Induced Wound in Albino Rats Pharmacological and Histological Comparative Study

Fady Sayed Youssef[1], Heba M. Fawzy[2], Sameh Hamed Ismail[3] and Gehad G. Mohamed[4,5]

[1] *Pharmacology Department, Faculty of Veterinary Medicine, Cairo University, 12211 Giza, Egypt.*
[2] *Histology and Cell Biology Department, Faculty of Medicine, Ain Shams University.*
[3] *Nanotechnology for postgraduate studies - Cairo University- Sheikh Zayed Branch Campus, Sheikh Zayed City, Giza PO 12588, Egypt.*
[4] *Chemistry Department, Faculty of Science, Cairo University, 12613, Giza, Egypt.*
[5] *Nanoscience Department, Basic and Applied Sciences Institute, Egypt-Japan University of Science and Technology, New Borg El Arab, Alexandria, 21934, Egypt.*

THIS work aims to fabricate two alternative nanoparticle formulas based on natural materials (*Astragalus polysaccharides*) as well as metallic materials (gold and silver nanoparticles), which represent quick, simple, and cost-effective approaches for improving the activity of the particles to promote wound healing. The Gold –silver and APS Nanocomposite gels were characterized by using Transmission Electron Microscope (TEM), Zeta potential, dynamic light scattering. The results revealed spherical to sub-spherical shape of the Gold-Silver nanocomposite gel without any aggregation and with homogeneous dispersion in the gel matrix was shown in TEM images. , dynamic light scattering demonstrated that the size were 85 nm and (30-50 nm) for Gold-Silver nanocomposite gel and *Astragalus polysaccharides* nano gel respectively. The excellent bioactivity of the Gold-Silver nanocomposite gel and the *Astragalus polysaccharides* nano gel was demonstrated by their respective zeta potential values of -25.2±0.71 mV and +30.4±1.65 mV. The generated nanocomposite gel's capacity for *in vivo* wound repair was assessed by histopathological confirmation and macroscopical images that showed the healing process. In comparison to Gold-Silver nanocomposite gel and the untreated control group Pharmacological investigations wound size histopathological investigations of the *Astragalus polysaccharides* treated group revealed significantly greater re-epithelialization, hair follicle regeneration and nearly normal α-SMA. The generated *Astragalus polysaccharides* nano gel has better wound healing capability when compared to Gold-Silver nanocomposite gel and the untreated groups, according to our results of the investigated pharmacological parameters by increasing the wound closure at the 15th day compared to other groups.

Keywords: Gold - Silver nanocomposite gel, *Astragalus polysaccharides* Nano Gel, Wound healing, TEM, Dynamic light scattering, Histopathological, Pharmacological.

Introduction

The construction of novel materials with dimensions between 1 and 100 nm has been considered a potential use of nanotechnology since 1974 [1]. The term "nano" comes from the Latin word "nanos," and 1 nm is equal to 10^9 m, as stated by Youssef et al. [2]. Nanotechnology is another recent advancement that spans several fields of study, such as medicine, agriculture, and the testing of anti-infective therapies. There is also the possibility that nanomaterials will affect in vivo and in vitro biomedical applications [3].

Nanoparticles' superior physicochemical properties over bulk materials include increased reactivity, larger surface area, greater stability, greater bioactivity and bioavailability, and the ability to regulate molecule size, drug delivery, and site-specific targeting [4].

*Corresponding author: Fady Sayed Youssef, E-mail: fadyalsalhany@cu.edu.eg., Tel.:01094572140
(Received 10/11/2023, accepted 03/12/2023)
DOI: 10.21608/EJVS.2023.247684.1668

Additionally, because nanoparticles can more easily penetrate cells, tissues, and organs than macroparticles can, they have variable applications in the field of medicine. The high toxicity and restricted bioaccessibility of current medications may be overcome through this. Drugs can be incorporated into or adhered to the surface of nanoparticles [5]. Nanotechnology's capacity to permeate cells, tissues, and organs better than full-scale particles might improve medication bioavailability and toxicity. Prescriptions can be fused within or on nanoparticles. Nanomedicine uses nanotechnology-based tools to solve scientific challenges and manage infections faster and more effectively [6].

The curiosity of freshly created atoms can lead to a novel pharmaceutical treatment that treats illnesses, protects animals from viral or bacterial infections, and speeds up wound healing. Additionally, these novel combinations might deliver medications into cells to treat ailments [7]. The integration of medications with diagnostics, known as nano-theragnostic, has been recognized as a treatment strategy. The primary objective of this approach is to enhance the efficacy and safety of drugs by closely monitoring the treatment response. Furthermore, they offer a valuable opportunity to design and develop combination agents that facilitate the delivery of therapeutics and the utilization of previously employed detection modalities throughout the treatment regimen [8]. The topic of nano pharmaceuticals is one of the most promising and fruitful areas of nanotechnology, and it offers a wide range of benefits to veterinary medicine [9].

Because of their great propensity to become infected by microorganisms, wounds are notoriously difficult for medical professionals to treat. In addition, there should be a focus on achieving rapid and adequate wound healing with a minimum of unattractive scarring. Nanotechnology is a burgeoning and more important field that has a vast number of applications in the field of biomedicine. These applications offer cutting-edge care for a variety of wounds [10].

The stems or dried roots of *Astragalus membranaceus* are traditional Chinese medicine used to make Astragalus polysaccharide (APS), a form of water-soluble heteropolysaccharide with medicinal properties [11]. APS has been widely used because of its low toxicity, adverse effects, lack of residue, and intolerance [12].

According to Yang et al.'s research, APS showed promise in treating diabetic skin lesions [13]. Therefore, current research suggests that APS may be crucial in controlling wound healing.

According to Sajjad and Nasseri [14], the synthesis of silver nanoparticles was accomplished by a variety of techniques, including precipitation, Sono chemical, and solvothermal processes. It has been reported that silver nanoparticles were effective on some bacteria like *E. coli, S. aureus, Klebsiella, and Pseudomonas* by attacking their respiratory chain and cell division, which resulted in cell death. Some nanoparticles, such as silver nanoparticles, at low concentrations, were nontoxic to humans.

Through the process of carboxymethylation modification, Pyun *et al.,* [10] were able to manufacture a partly carboxymethylated cotton gauze (PCG) containing Ag-NPs. The cell survival and cell attachment studies demonstrated that the nanocomposite was not cytotoxic and promoted wound healing in an animal model. This was demonstrated by the fact that the nanocomposite was successful.

It was reported by Masood *et al.,* [15] that the manufacture of Ag-NP-impregnated hydrogels of chitosan–polyethylene glycol (PEG) enhanced the wound healing process in diabetic wound-caused rabbits. When compared to neat hydrogels, their findings indicated that Ag-NP-impregnated hydrogels had a greater degree of porosity, a larger rate of swelling degree, and a transition of water vapor.

The aim of our study was to prepare and characterize APS Nano gel and Gold-silver Nanocomposite gel are prepared and characterized for wound healing function.

Material and Methods

The materials

No purification is required for any of the chemicals, since they are lab-grade. Sigma Chemical Co. manufactures silver nitrate ($AgNO_3$), gold chloride, trisodium citrate (TSC), and carbopol 940. In order to extract the APS (dried root of superior quality), the root of Astragalus membranaceus was used (Qi Jing Ltd, Beijing, China).

Methods

Synthesis of silver nanoparticles

The manufacture of silver nanoparticles involved the utilization of silver nitrate and trisodium citrate as precursor materials. The silver colloid was generated through the utilization of the co-precipitation process. In a standard experimental procedure, a volume of 50 mL of a 0.001 M $AgNO_3$ solution was subjected to heating until it reached its boiling point. Subsequently, a 5 mL portion of a 1% trisodium citrate solution was incrementally introduced into the mixture by a dropwise method. Throughout the experiment, the solutions were forcefully mixed and subjected to heat until a noticeable color change, specifically a pale yellow, was observed. Subsequently, the substance was extracted from the heating apparatus and agitated until it reached ambient temperature. It was then carefully transferred into

opaque containers to prevent any potential influence from light exposure [14].

Synthesis of gold nanoparticles

However, gold nanometal was synthesized by the co-precipitation method. In a typical synthesis, gold chloride (source material) and trisodium citrate (precipitating agent) were used to synthesize gold nanometal according to the Turkevich method [16]. With some modification from the authors, gold nanometal was prepared by dissolving 0.002 mM of gold chloride in 70 mL of (de-ionized distilled water) then 0.2 M of trisodium citrate was added dropwise. The mixture was subjected to ultra-sonication using a prop sonicator (Hielscher UP400S, 400 W, 24 kHz, an amplitude of 60% and a cycle of 0.5) for 15 minutes at a temperature of 90 °C. The colloidal pink color of gold nanometal was obtained.

Synthesis of Gold-Silver Nanocomposite Gel:

The synthesis of a gold-silver nano-gel. In the standard protocol, a solution containing 0.75 g of Carbopol 940 was prepared by dissolving it in 350 ml of doubly deionized water. This solution was then combined with 100 milliliters of silver nanoparticles at a concentration of 50 ppm, along with 50 ppm of gold. The mixture was subjected to sonication using a Hielscher Company model up 400s sonication device, with an amplitude of 71 and a cycle of 91%. Subsequently, 75 ml of trimethylamine was added dropwise to the mixture while continuous sonication was maintained, resulting in the formation of a pale-yellow gel.

Synthesis of *Astragalus membraneceus polysaccharides* Nano gel

Astragalus membraneceus polysaccharides were previously prepared and characterized by one of our authors according to the method described by Ramadan *et al.,* [17]. The usual approach for synthesizing APS nano-gel involves the preparation of a solution of 0.75 g of Carbopol 940 dissolved in 350 ml of doubly deionized water. Subsequently, the aforementioned solution was amalgamated with 100 milliliters of APS, possessing a concentration of 50 parts per million (ppm). The mixture underwent sonication using a Hielscher Company type-up 400s sonication equipment, with an amplitude of 71 and a cycle of 91%. Following that, a volume of 75 ml of trimethylamine was gradually added to the mixture under constant sonication, leading to the gel formation.

Characterization

The purpose of this study is to evaluate the wound-healing capabilities of Gold - Silver nanocomposite gel and APS Nano Gel. The specimens have been indexed, identified, and microscopically characterized. By using the TEM (Transmission Electron Microscopy) model of Jeol, JEM-2100 high-resolution, Japan, it was possible to determine the surface topography and shape of APS Nano Gel and Gold - Silver Nanocomposite gel. DLS (dynamic light scattering) (Malvern, UK) facilitates the identification of dispersion in solution by zeta potential and sizing.

Animals (care, housing, preparation, and design)

This study enrolled on forty adult female albino rats, their weight and age were (150 - 200). A mesh wire cover was placed over the cages to protect them from the elements. For the duration of the experiment, the rats were fed a rat chow diet and given Add libitum tab Water.. A proper temperature, light, and humidity environment was provided for them. Egyptian organization of biological products and vaccines (Cairo, Egypt), the animal house of Cairo University-Egypt Department of Pharmacology, provided the rats.

Animals (care, housing, preparation, and design)

This study enrolled on forty adult female albino rats, their weight and age were (150 - 200). A mesh wire cover was placed over the cages to protect them from the elements. For the duration of the experiment, the rats were fed a rat chow diet and given Add libitum tab Water.. A proper temperature, light, and humidity environment was provided for them. Egyptian organization of biological products and vaccines (Cairo, Egypt), the animal house of Cairo University-Egypt Department of Pharmacology, provided the rats.

Ethical Approval

The study was approved by the Institutional Animal Care and Use Committee (IACUC) with approval No. Vet CU 03162023734.

Experimental design

After seven-day acclimatization period, rats were randomly divided into four groups 10 rats each:

I. Control group in which rats received only food and water.

II. Wounded untreated group.

III. APS Nano: wounded group that was treated with APS nano gel daily applied to the wound area.

IV. Gold-silver Nanocomposite: wounded group that was treated with gold-silver Nanocomposite gel daily applied to the wound area.

The procedure of full-thickness skin wound

A 40 mg/kg intraperitoneal injection of pentobarbital sodium was used to anesthetize the rats before and during wound excision [18]. Routine preparation was done to all experimental animals An electric clipper was used to shave all animals' dorsal fur, and 70% alcohol was used to disinfect it. Each rat was excised with a circular wound of

approximately 100 mm^2 on the dorsal side at the same time taking care not to injure the muscle layer as described by El Banna *et al.,* [19].

Day zero begins on the day of wounding. On days 0, 3, 9, 12, and 15 after wounding, wound size closure (mm) was assessed macroscopically on each of the four groups of animals (I, II, III, IV). Drugs were applied topically every day till day 15 of the experiment.

Parameters for evaluation of wound healing in different groups

In addition to a photomicrograph of collagen bundles in different groups, a histological evaluation of wound healing size (mm) along the duration of treatment (0, 3, 9, and 15), and a histopathological evaluation of wound healing percentages were all conducted **[20]**.

Histopathological examination

Skin Specimens were collected on day 15 post-surgery and conserved in a solution of 10% neutral buffered formalin. Subsequently, these samples underwent standard procedures for processing, For staining and examination, a light microscope was used. Based on the methodology, histological lesion scores were determined as described by Hosseini *et al.*, [21]. Additionally, further tissue slides were subjected to staining using Masson's trichrome stain (MTC) to assess the deposition of collagen fibers in the dermal layer. The quantification and statistical analysis of collagen fibers were conducted based on their area %. And on their maturity because the immature collagen tissue show more cellularity while mature one have low cellular content.

Immunohistochemical staining of α-SMA

The sections were deparaffinized, rehydrated, and covered with H_2O_2 for 15 minutes. Antigen retrieval was performed by immersing them in citrate buffer solution and microwaved them for 10-20 minutes. The slides were washed, incubated in normal blocking goat serum, and covered with 50-80 µl of primary α-SMA antibody overnight. The slides were then incubated with a secondary biotinylated anti-mouse antibody for 30 minutes, washed, and blotted. Slides were covered with streptavidin and horseradish peroxidase conjugate, washed with PBS, and added with DAB. After blotting, counterstained with Gill hematoxylin, washed, dehydrated, and mounted. The positive reaction resulted in brown actin filament coloration. No reaction was detected in the negative control run **[22]**.

Statistical analysis

Data were analyzed using IBM SPSS statistics 20 software using one-way analysis of variance (ANOVA) followed by the Duncan multiple comparisons test for post hoc analysis. A $p<0.05$ was considered statistically significant. Non-significant when the P value was > 0.05. Values were expressed as mean ± SD.

Results and Discussion

Characterization

Transmission Electron Microscope (TEM)

TEM images of the created gold-silver Nanocomposite gel illustrated that the resulting particles are spherical to sub-spherical structures in the form of clusters with a maximum thickness of about 70-90 nm Fig (1a). Additionally, it was shown that APS Nano gel particles are spherical and purified without any agglomeration. Fig. (1_b).

Zeta size and potential

Gold-silver Nanocomposite gel and APS Nano gel nanoparticles have spherical morphologies in TEM images, suggesting a uniform dispersion within the gel matrix and no aggregation. The size of the gold-silver Nanogel and APS Nanogel was determined using the dynamic light scattering (DLS) technique, resulting in readings of 85 nm and (30-50 nm) respectively. Nevertheless, it is important to acknowledge that the DLS measurements do not correspond with the findings obtained using transmission electron microscopy (TEM) as a result of the gel material's effective coating. The zeta potential values of the Gold-Silver Nanocomposite gel and APS nano-gel were determined to be -25.2±0.71 mV and +30.4±1.65 mV, respectively. The findings of this study demonstrate a notable degree of bioactivity in both gel formulations.

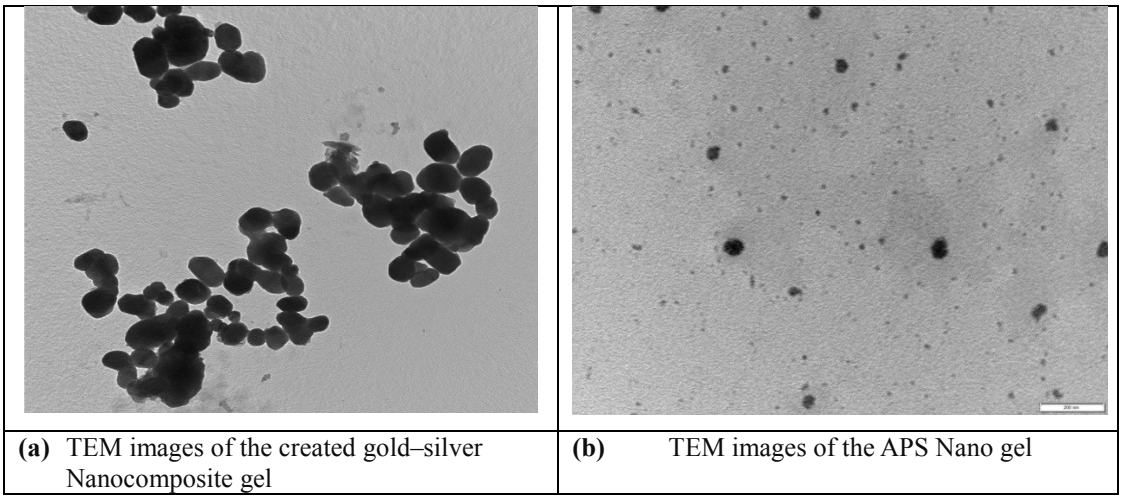

(a) TEM images of the created gold–silver Nanocomposite gel

(b) TEM images of the APS Nano gel

Fig.1. Showing transmission electron microscope of Gold Silver Nanocomposite gel (a) and APS Nano gel (b).

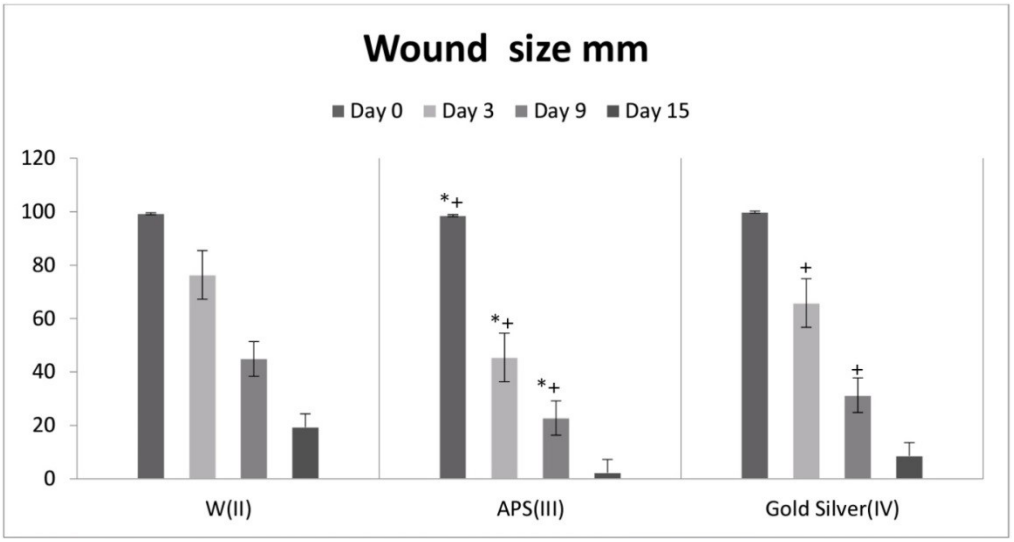

Fig. 2. On days 0, 3, 9, and 15, wound size was measured in different study groups.

Effect of APS Nano gel and Gold silver nano gel on wound healing. Data are presented as means ± SEM. significance is considered at P <0.05 (n = 10 rats/group). * $p < 0.05$ compared to the control wounded group and + $p < 0.05$ compared to Gold silver nano gel treated group.

Wound size

All experimental groups did not show a significant difference in wound healing closure at day 0. In comparison with the non-treated group (II), the groups receiving Nanocomposite (group III and group IV) showed higher wound closure (mm^2). On day 15, the wound healing speed of the APS Nano gel group was significantly faster than that of the other groups. Compared to other treated groups, non-treated group II showed slower wound healing at 3, 9, and 15 days after induction (**Fig. 2**).

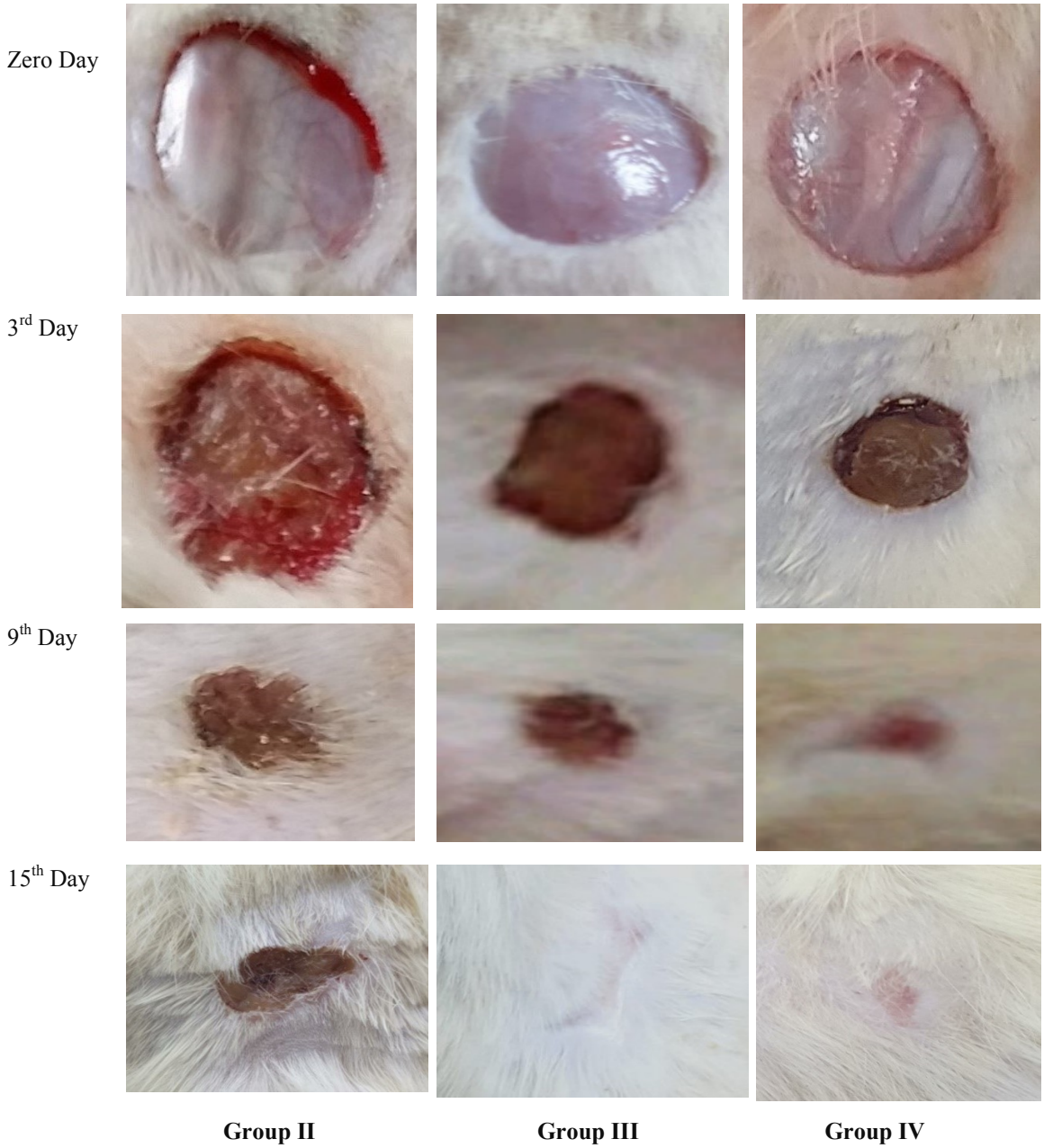

Fig. 3. Macrophotography exhibited experimental wounded full thickness of skin at different period of treatment groups (Group II: Group of wounds without treatment, Group III: A group of wounds treated with APS, Group IV: wound group treated with gold-silver nanocomposite.

Histopathological examination

In the control group, thin sections of skin stained in H & E revealed that the epidermis and dermis, the two layers of skin. The epidermis was stratified squamous keratinized epithelium. Dermis was formed by the application of connective tissue in layers, with no clear demarcation line, in which hair follicles are located in the deep thick reticular layer (Figs. 4A, IB). At the site of the wound, At the day 15 of experiment, epidermal loss was observed on thin skin sections from group II. The granulation tissue was composed of collagen fibers full of mononuclear inflammatory cells and fibroblast. In addition to the large number of fat cells (Figs. 4C, ID). Sections of skin from group III revealed a complete coverage of the epidermis over the wound site (Figs. 4E, IF). Examination of group IV sections revealed a thin, newly produced epidermis covering the location of the wound. Few layers of flattened, undifferentiated cells made up the newly created epidermis, which was separated from the underlying dermis in certain places. The dermis was devoid of hair follicles and loaded with mononuclear inflammatory cells. (Figs. 4G, IH). An apparent increased thickness of the epidermis was noticed in group III compared to group IV.

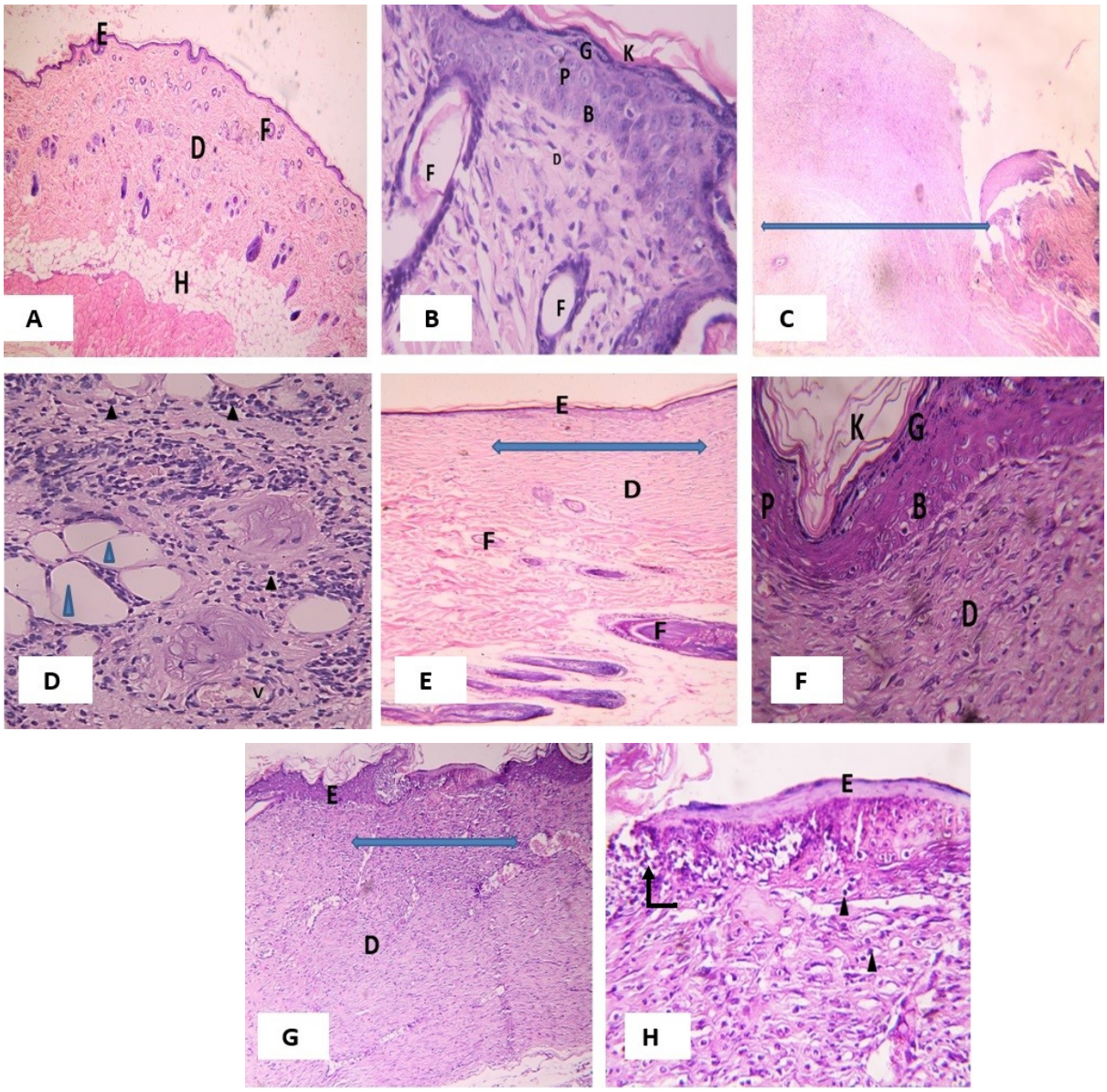

Fig. 4. Photomicrographs of sections in the thin skin of rats from different groups (Day 15) (A, B) control group;(C, D) group II ; (E, F) group III ; (G, H) group IV. Basal cell layer of the epidermis (B), prickle cell layers (P), granular cell layers with basophilic granules (G) horny layers (K) of the epidermis, dermis (D), hypodermis(H), hair follicles (F) wound area(↔); separation between dermis and epidermis (elbow arrow);.mononuclear inflammatory cells(►)fat cells(blue ►) H and E [A, C, E, G X100], [B, D, F, H X 400].

When Masson's trichrome stained the papillary dermis of the control group, thin interlacing collagen fibers were visible, whereas the reticular dermis had coarse, wavy collagen fibers (Figs. 5A, 5B). In the slices from group II, mononuclear inflammatory cells and fine collagen fibers could be seen throughout the granulation tissue (Figs. 5C, 5D). Collagen fibers with low cellular were more organized in group III at the wound site compared to group II, but spaces were occasionally visible between collagen fibers (Fig. 5E) with the reappearance of hair follicles. Group IV's underlying dermis displayed aberrant collagen organization at the wound site. Both papillary and reticular dermis was formed of fine interlacing collagen fibers (Fig. 5F).

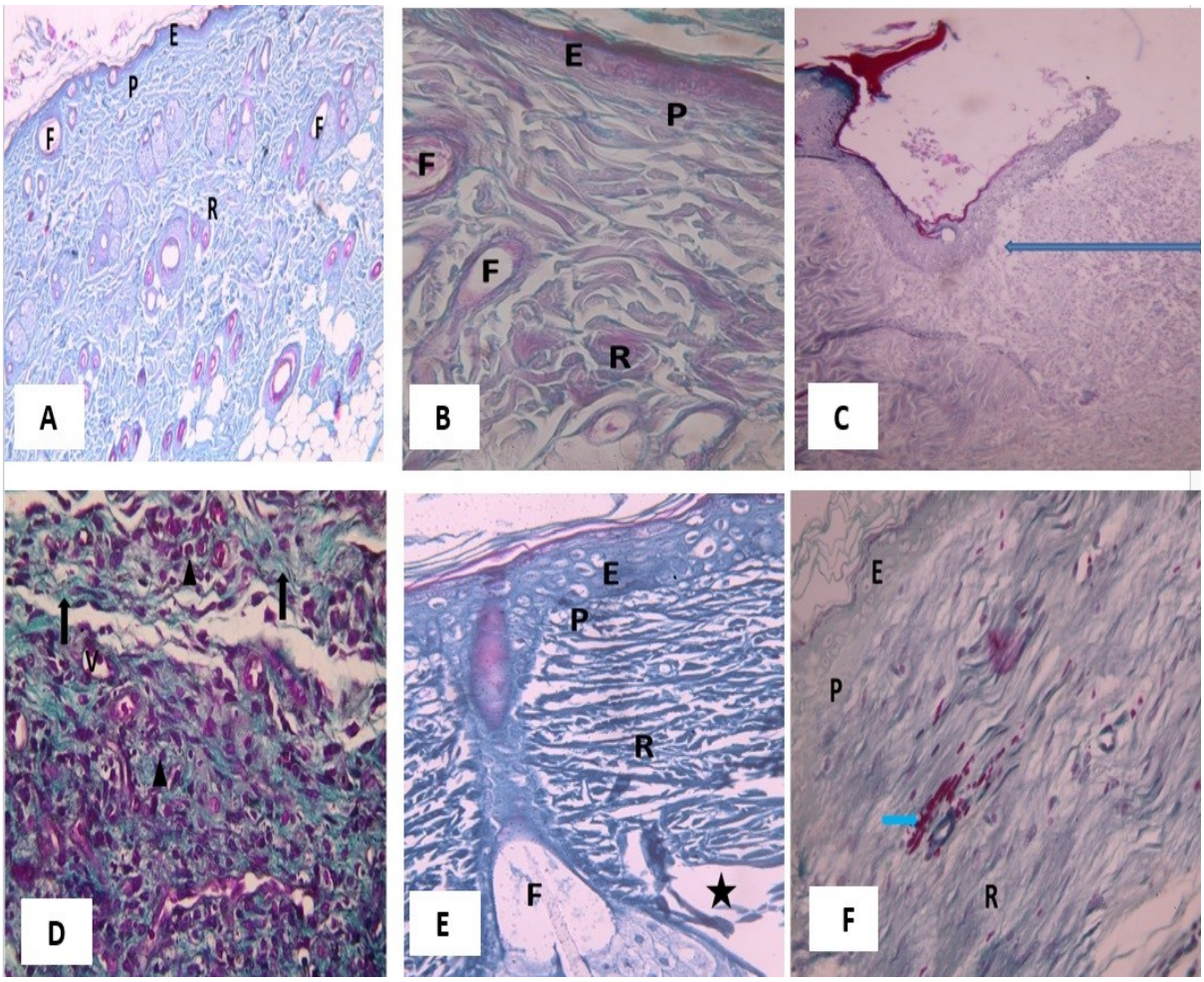

Fig. 5. photomicrographs of sections in the thin skin of different groups (Day 15): (A, B) control group;(C, D) group II ; (E) group III ; (F) group IV. Epidermis (E); papillary dermis (P), reticular dermis (R), numerous mononuclear inflammatory cells (►), fine collagen fibers (↑)in the granulation tissue extravasated blood(blue↑).spaces in between collagen fibers( ), hair follicle(F). (Masson's trichrome stain [A, C X100] [B, D, E, F X400].

Immunohistochemical staining for α-SMA revealed a strong positive cytoplasmic immune reaction in the wall of blood vessels of the dermis. The blood vessels appeared with a thin wall and patent lumen in the control group (Fig. 6A). A strong positive reaction was found in both dermal blood vessels, as well as many connective tissue cells in group II, most likely dermal myofibroblasts which appeared branched and parallel to the skin surface (Figs. 6B, 6C), group III showed positive reaction in dermal blood vessels that was comparable to control (Fig. 6D). In group IV positive reaction of α-SMA appeared both in the wall of dermal blood vessels as well as the dermal myofibroblasts. (Fig. 6E).

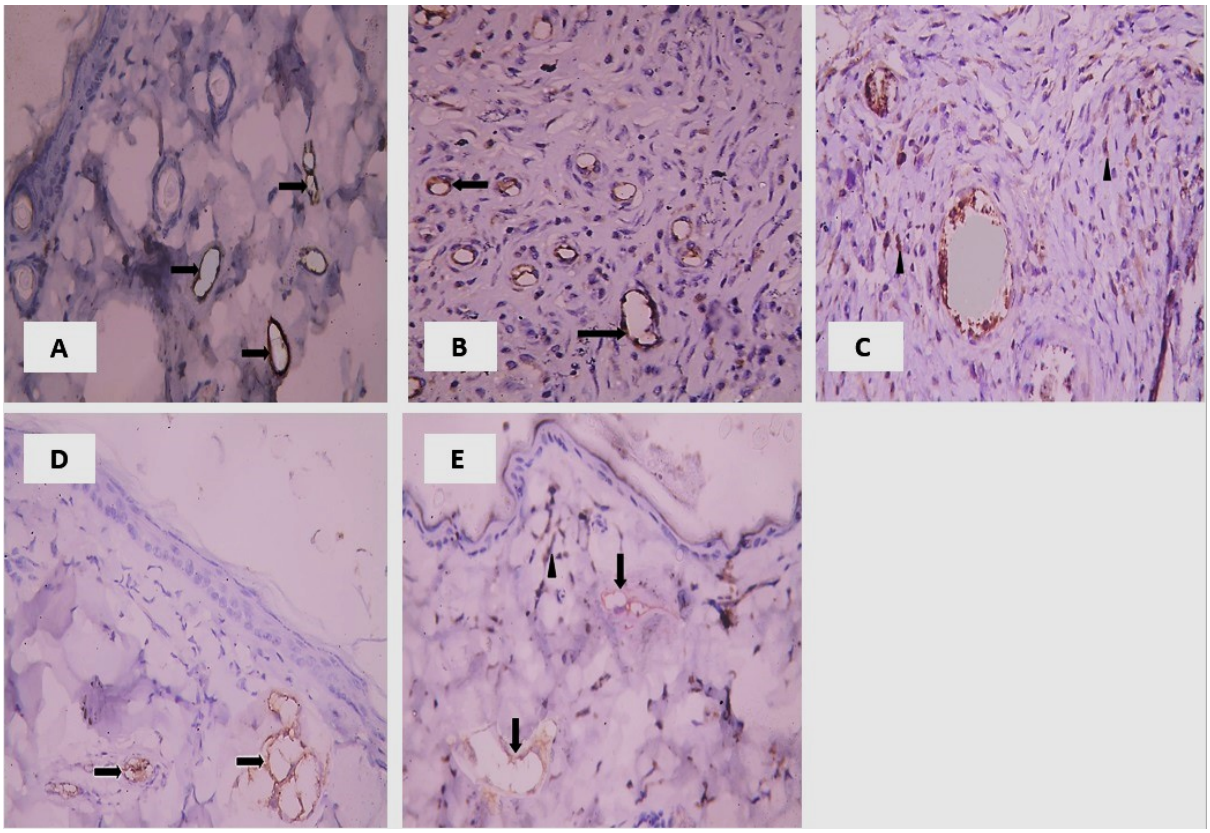

Fig. 6. Photomicrographs of sections in rat's skin from different groups (Day 15): (A) control group;(B, C) group II;(D) group III;(E) group IV. Positive reaction for α- SMA in the wall of dermal blood vessels (↑); positive reaction for α-SMA connective tissue cells in the dermis (►) (Streptavidin-biotin peroxidase for α-SMA x 400).

TABLE 1.Morphometric and Statistical results

Groups	Control	Group II	Group III	Group IV
Epidermal thickness	48.14 ±3.01	0.00 **(■) (●) (*)**	46.36 ± 4.01	40.15 ± 1.87 **(■)**
Collagen area %	31.76 ± 3.92	10.23± 2.19 **(■)(●) (*)**	26.88 ± 1.34	21.18 ± 3.15 **(■)**
α- SMA density	70.21 ± 1.2	84.43 ± 1.63 **(■) (●) (*)**	67.53 ± 3.13	64.53 ± 2.73

Table (1) Showing the mean ± SD of Epidermal thickness, the area percentage of collagen in the dermis, and α-SMA in the different groups and their relation.

(■) significance of difference by LSD from group I ($P < 0.05$)

(●) significance of difference by LSD from group III($P < 0.05$)

(*) significance of difference by LSD from group IV($P < 0.05$)

The complex process of wound healing requires the interaction of several cells and mediators over a very long period [23].

In this study, we synthesized two natural and metallic nanoparticle formulas utilizing fast, cheap, and easy approaches to aid wound healing. Gold-silver nanoparticle gel was the first recipe. The second similar product was an Astragalus polysaccharide nanogel. The nanocomposite gel was studied by TEM, Zeta potential, and DLS. The nanocomposite gel's in vivo wound-repairing ability was tested. Histopathological confirmation and macroscopical photographs of wound healing were used to evaluate healing. TEM pictures demonstrate the spherical Gold-Silver nanocomposite gel without aggregation and homogenous gel matrix dispersion. The Gold-Silver nanocomposite gel and APS nano gel's zeta potential values of -25.2±0.71 mV and +30.4±1.65 mV showed their high bioactivity. Histological research showed that APS-treated skin had higher re-epithelialization and skin structure regeneration than Gold-Silver Nano gel and the untreated groups. A normal α-SMA confirmed this. According to our parameter data, APS nano gel may cure wounds better than Gold-Silver nanocomposite gel and the untreated groups.

In untreated rats after 15 days of wound induction (Groups II), epidermal loss was observed. Fibrous content and many inflammatory cells make up the granulation tissue. The granulation tissue also showed the appearance of fat cells.

Our findings support a previous study's finding of Henry and Garner [24], that an injured site would undergo inflammatory cell infiltration following the formation of a stable clot in the dermal tissues. They added that the first inflammatory cells to reach the wound site to kill germs and start the inflammatory process are neutrophils. Mercandetti and Cohen [25] added that, a variety of cells, including inflammatory cells, fibroblasts, myofibroblasts, and endothelial cells, can be found in granulation tissue. Collagen, extracellular matrix, blood vessels, and granulation tissue also contain extracellular matrix. This position will change as the body matures and remodels.

Plikus *et al.* [26] found that Adipocytes may play a role in tissue repair through transdifferentiation of myofibroblasts after skin damage. It has been shown that fibroblast migration and matrix deposition are impaired when adipocyte precursor cells are prevented from forming, which can lead to the development of mature adipocytes. Myofibroblasts have been shown to transdifferentiate into adipocytes after skin damage, suggesting that adipocytes may play a role in tissue repair [26]. As a consequence of the preventive development of adipocyte precursor cells, defects in fibroblast migration and matrix deposition arise. Adipocyte precursor cells differentiate into mature adipocytes, which appear to play a role in repair and regeneration [27].

Immune staining of α- SMA showed a significant increase in group II. The differentiation of fibroblasts into myofibroblasts, which are distinguished by alpha-smooth muscle actin (α -SMA), occurs in response to TGF- β1 stimulation [28].

Putra *et al.* [29] added, that granulation tissue began to grow gradually approximately a week after wounding and was identified by myofibroblast-expressed α -SMA**.** According to Chaudhuri *et al.,* [30], additional potential sources of myofibroblasts under the influence of TGF- β1 include the pericytes or vascular smooth muscle cells that surround blood vessels, microvascular endothelial cells, and bone marrow cells.

In the APS-treated group (Group III), differentiated keratinocytes formed a new epidermis covering the site of the wound. Keratinocytes were present in normal layers. It contained keratohyalin granules, demonstrating maturation of the stratum granulosum. Similar results were detected by Yang *et al.,* [31] who used an APS-loaded scaffold in the treatment of diabetic wounds, they found Higher APS loading in a scaffold resulted in earlier and better skin microcirculation restoration as well as quicker wound healing. This favorable impact of APS-loaded scaffold on skin tissue regeneration in diabetic rats may have resulted not only from imitating extracellular matrix ultrastructure but also from restoring the microcirculation of the skin illustrating our finding of comparable α –SMA expression of this group to the control group.

Putra *et al.,* [32] demonstrated that α –SMA expression correlates with wound closure, in which TGF-β induce the α-SMA expression that align parallel to mechanical tension in granulation tissues.

Another study suggested that the new polysaccharide APS2-1, reduced inflammation, promoted cell division, and increased the release of repair components, had a high potential for aiding in wound healing. **[33].** APS effects on granulation tissue demonstrate some spaces between mononucleate inflammatory cells, fibroblasts, and collagen fibers in group III of the present study. Fibroblasts are deposited into the wound bed during the initial stages of wound healing and generate collagen to facilitate migration to the wound site. The formation of collagen is crucial because it strengthens the wound. Skin has a large amount of type-I and type-III collagen. In the proliferation and maturation phases of the wound healing process, weaker type-I collagen replaced collagen-III, which first emerged. The results of the investigation showed that collagen thickened towards the end of the healing process [34].

During week 3, the maturational or remodeling phase begins. It may last up to 12 months. As the wound contraction peaks around week 3, the extra collagen dissolves and the wound becomes less inflamed. Secondary healing is markedly more likely to produce wound contractions than primary healing. Incision wounds reach their maximum tensile strength between 11 and 14 weeks. Thus, collagen degradation may illustrate spaces that exist between collagen fibers [35].

Another explanation for spaces found in between collagen fibers was made by Alhajj and Goyal [36] who referred this to presence of new vessels formed during angiogenesis which are leaky. This leakiness explains why granulation tissue is often edematous, and accounts in part for the edema that may persist in healing wounds long after the acute inflammatory response has resolved.

When the Silver-Gold nanocomposite-treated group (Group IV) was examined, it revealed that the wound region had just developed a thin epidermis made of flattened, undifferentiated keratinocytes. with underlying dermis loaded with mononuclear cellular infiltration. Xiao *et al.* [37] referred undifferentiated epithelium to overproduction of proinflammatory cytokines which is harmful and may lead to dysregulated epidermal stem cell activation and differentiation.

While Nam *et al.,* [35], reported that, the application of nanocomposites dissolved in silver molecules,has been shown to improve the healing process by directly expressing collagen and some growth factors, which leads to re-epithelialization, vasculogenesis (neovascularization), and the accumulation of collagen fibers. It has further been demonstrated that silver nanoparticles can increase the number of keratinocytes and encourage them to migrate to the wound center, as well as induce differentiation of fibroblasts into myofibroblasts, which can facilitate wound healing. You *et al.,* [38], According to research, several nanoparticles can help fibroblasts migrate from the wound edge, which promotes remodeling by increasing alpha-smooth muscle actin levels. A further theory was that nanoparticles accelerate wound healing by inhibiting bacterial growth and releasing pro-inflammatory cytokines.

Baygar *et al.* [39] It has been shown that an increase in AgNP in the dressing results in a smaller wound area and increased collagen deposition linked to macrophage and fibroblast migration. Two characteristics contribute to gold nanoparticles' antibacterial spectrum: their ability to discharge metal ions and their unique nature [40].

Pormohammad and Turner [41] stated that, A synthetic metal with an effective antimicrobial spectrum, gold salt (tetrachlorocuprate (III) trihydrate) is used to produce gold alloy. It is only the high cost of gold nanoparticles (AuNPs) that limits their application in wound healing due to their limited cytotoxicity. Combined with collagen, AuNPs show skin wound healing properties in a dose-dependent manner due to their anti-inflammatory and antioxidant properties. Additionally, AuNPs promote collagen regeneration and enhance wound healing through their anti-oxidative and anti-microbial properties. Due to inadequate time, the wounds didn't enter the maturational or remodeling phase, despite the presence of fine interlacing collagen fibers [42].

Our results were worse than the previous study of Fawzy *et al.* [43] when using silver nanoparticles alone. **Abd el** Dayem *et al.* [44] demonstrated that Cells can protect themselves from nanoparticles at low concentrations, and antioxidant activity reduces oxidative damage and returns the redox equilibrium. Higher quantities, however, render this mechanism of action impossible and result in cell toxicity and inflammation and this illustrates our findings of the presence of highly cellular dermis in this group.

Talaraska *et al.,* [45] added that reactive oxygen species generation has also been linked to an increase in the toxicity of nanoparticles. Ag nanoparticles enter the cell and break down inside, generating Ag+ ions that damage the mitochondria. Apoptosis eventually results from ROS, which build up as byproducts of the electron transport chain and damage and impair the function of mitochondria, depolarize the mitochondrial membrane, and damage mtDNA (mitochondrial DNA).

Conclusions

As compared to untreated rats and silver - Gold silver-nanocomposite-treated rats, APS-treated rats demonstrated significantly more re-epithelialization and dermal structural regeneration.

Conflict of interest

There are no declared conflicts of interest. The corresponding author is ready to provide any detailed data upon request.

Acknowledgement: Not applicable

Funding statement: Not applicable

Author`s contributions:

Dr. Fady: synthesized the nanomaterial, initiated & applied the pharmacological experimental design, collected the samples and interpreted the results
Dr. gehad & Dr.sameh: Characterized the nanomaterials
Dr Heba: Histopathological examination.

References

1. Youssef, F. S., Elbanna, H. A., Elzorba, H. Y., Galal, A. M., Mohamed, G. G. and Ismail, S. H. Synthesis and characterization of florfenicol-silver nanocomposite and its antibacterial activity against some gram-positive and gram-negative bacteria. *International Journal of Veterinary Science*, **9**(3), 324-330(2020).

2. Youssef, F., Mohamed, G., Ismail, S., Elzorba, H., Galal, A. and Elbanna, H. Synthesis, characterization and in vitro antimicrobial activity of florfenicol-chitosan nanocomposite. *Egyptian Journal of Chemistry*, **64**(2), 941-948(2021).

3. Youssef, F. S., Ismail, S. H., Fouad, O. A. and Mohamed, G. G. Green synthesis and Biomedical Applications of Zinc Oxide Nanoparticles. Review. *Egyptian Journal of Veterinary Sciences*, **55**(1), 287-311(2024).

4. El-Banna, A. H., Youssef, F. S., Youssef Elzorba, H., Soliman, A. M., Mohamed, G. G., Ismail, S. H. and Osman, A. S. Evaluation of the wound healing effect of neomycin-silver nano-composite gel in rats. *International Journal of Immunopathology and Pharmacology*, **36**, 03946320221113486 (2022)**.**

5. Ramadan, R. M., Youssef, F. S., Mohamed, G. G., Ismail, S. H., El-Bahy, M. M. and Abdel-Radi, S. Synthesis, characterization and investigation of the anti-coccidial activity of new formulation curcumin-olive oil nanocomposite. *Advances in Animal and Veterenary. Sciences*, **10**(10), 2186-2196 (2022) **.**

6. Taha, N. M., Abdel-Radi, S., Youssef, F. S., Auda, H. M., El-Bahy, M. M. and Ramadan, R. M. Parasiticidal Efficacy of a New Formulation of Silver Nanoparticles on *Trichinella spiralis* in vitro. *Journal of Advanced Veterinary Research*, **12**(4), 379-385 (2022).

7. Ramadan, R. M., Youssef, F. S., Fouad, E. A., Orabi, A. and Khalifa, M. M. The pharmacological impact of Astragalus membranaceus against coccidial and bacterial infection in vitro. *Egyptian Pharmaceutical Journal*, *22*(2), 324 (2023).

8. Khalifa, M. M., Ramadan, R. M., Youssef, F. S., Auda, H. M., El-Bahy, M. M. and Taha, N. M. Trichinocidal activity of a novel formulation of curcumin-olive oil nanocomposite in vitro. *Veterinary Parasitology: Regional Studies and Reports*, **41**, 100880 (2023).

9. Youssef, F. S., El-Banna, H. A., Elzorba, H. Y. and Galal, A. M. Application of some nanoparticles in the field of veterinary medicine. *International Journal of Veterinary Science and Medicine*, **7**(1), 78-93 (2019).

10. Pyun, D. G., Yoon, H. S., Chung, H. Y., Choi, H. J., Thambi, T., Kim, B. S. and Lee, D. S. Evaluation of AgHAP-containing polyurethane foam dressing for wound healing: synthesis, characterization, in vitro and in vivo studies. *Journal of Materials Chemistry B.*, **3**(39), 7752-7763 (2015).

11. Li, C., You, P. M., Wang, C. X., He, J. X., Xiao, W. Y. and Guo Z. Research Progress on the Molecular Mechanism of Antioxidation of Astragalus Polysaccharide. *Journal of Minzu University China,* **40** (04), 78–82 (2019). 10.3969/j.issn.1009-2102.2019.04.014.

12. Jaheen, A. H., Youssef, F. S., Ali, M., El-sherif, M. and Oraby, M. O. H. A. M. E. D. Altered Hematological and Selected Serum and Rumen Constituents of Egyptian Rahmani Sheep Fed on Dried Chinese Herbal Astragalus Membranaceus Root Extract Supplemented Ration. *Egyptian Journal of Veterinary Sciences*, **54**(6), 1029-1039 (2023).

13. Y. Yang, F. Wang, D. Yin, Z. and Fang L. Huang, Astragulus polysaccharide-loaded fibrous mats promote the restoration of microcirculation in/around skin wounds to accelerate wound healing in a diabetic rat model, Colloids and Surfaces. *B, Biointerfaces*, **136**, 111–118 (2015).

14. Erdoğan, Meryem Kalkan. Preparation and stabilization of Ag nanoparticles with N-vinyl-2-pyrrolidone grafted-poly (vinyl alcohol) in an organic medium and investigation of their usability in the catalytic dye decolorization. *Colloid and Interface Science Communications*, **34**,100222. (2020).

15. Masood, N., Ahmed, R. and Tariq, M. Silver nanoparticle impregnated chitosan-PEG hydrogel enhances wound healing in diabetes induced rabbits. *International Journal of Pharmaceutics*, **559**, 23–36 (2019).

16. Turkevich, J., Stevenson, P. C. and Hillier, J. The formation of colloidal gold. *The Journal of Physical Chemistry*, **57**(7), 670-673 (1953).

17. Ramadan, R. M., Youssef, F. S., Fouad, E. A., Orabi, A. and Khalifa, M. M. The pharmacological impact of Astragalus membranaceus against coccidial and bacterial infection in vitro. *Egyptian Pharmaceutical Journal*, **22**(2), 324 (2023).

18. Gaertner, D.J., Hallman, T.M., Hankenson, F.C. and Batchelder, M.A. "Anesthesia and Analgesia in Rodents. Anesthesia and Analgesia in Laboratory Animals. Second Edition", *Academic Press*, CA, (2008).

19. El Banna, H., El Zorba, H. and Hossny, A. Comparative efficacy of grotto cream with fucidin cream on normal and diabetic wound models in rats. *Indian Journal of Physiology and Pharmacology*, **62** (1), 80–86 (2018).

20. Bakr, R. O., Amer, R. I., Attia, D., Abdelhafez, M. M., Al-Mokaddem, A. K., El Gendy, A. N., El-Fishawy, A. M., Fayed, M. A. A. and Gad, S. S. In-vivo wound healing activity of a novel composite sponge loaded with mucilage and lipoidal matter of Hibiscus species., *Journal of .Bio-Pharma*, **135**, 111225 (2021).

21. Hosseini, S. V., H., Niknahad, N., Fakhar, A., Rezaianzadeh, A. and Mehrabani, D. The healing effect of mixture of honey, putty, vitriol and olive oil in Pseudomonas aeroginosa infected burns in experimental rat model. *Asian Journal of Animal and Veterinary Advances*, **6**(6), 572–579 (2011).

22. Popescu, F.C., Busuioc, C.J., Mogoşanu, G.D., Pop, O.T., Pârvănescu, H., Lascăr, I., Nicolae, C.I. and Mogoantă, L. "Pericytes and myofibroblasts reaction in experimental thermal third degree skin burns". *Romanian Journal of Morphology and Embryology*, **52**(3), 1011-1017 (2011).

23. Sorg, H., Tilkorn, D. J. Hager, S., Hauser, J. and Mirastschijski, U. "Skin wound healing: an update on the current knowledge and concepts. *European Surgical Research*, **58**(1-2), 81–94 (2017).

24. Henry, G. and Garner, W.L. Inflammatory Mediators in Wound Healing. *Surg. Clin. N. Am.,* **83**, 483–507 (2003).

25. Mercandetti, M.; Cohen, A.J. Wound Healing and Repair. Available online: https://emedicine.medscape.com/article/1298129 (2008).

26. Plikus, M.V., Guerrero-Juarez, C.F., Ito, M., Li, Y., Dedhia, P.H., Zheng, Y., Shao, M., Gay, D.L., Ramos, R. and His, T.C. Regeneration of fat cells from myofibroblasts during wound healing. *Science*, **355**, 748–752 (2017).

27. Schmidt, B.A. and Horsley, V. Intradermal adipocytes mediate fibroblast recruitment during skin wound healing. *Development,* **140**, 1517–1527 (2013).

28. Klingberg, F., Hinz, B. and White, E.S. The myofibroblast matrix: implications for tissue repair

and fibrosis. *The Journal of Pathology*, **229** (2), 298-309 (2013).

29. Putra, A., Alif, I., Hamra, N., Santosa, O., Kustiyah, A.R., Muhar, A.M. and Lukman, K. MSC-released TGF-β regulate α-SMA expression of myofibroblast during wound healing. *Journal of Stem Cells & Regenerative Medicine*, **16**(2), 73-79 (2020). doi: 10.46582/jsrm.1602011. PMID: 33414583; PMCID: PMC7772809.

30. Chaudhuri, V., Zhou, L. and Karasek, M. Inflammatory cytokines induce the transformation of human dermal microvascular endothelial cells into myofibroblasts: a potential role in skin fibrogenesis. *Journal Cutan. Pathol.,* **34**,146–155(2007).

31. Yang, Y., Wang, F., Yin, D., Fang, Z. and Huang, L. Astragulus polysaccharide-loaded fibrous mats promote the restoration of microcirculation in/around skin wounds to accelerate wound healing in a diabetic rat model. *Colloids Surf. B Biointerfaces,* **136**, 111-118 (2015).

32. Putra, A., Alif, I., Hamra, N., Santosa, O., Kustiyah, A.R., Muhar, A.M. and Lukman, K. MSC-released TGF-β regulate α-SMA expression of myofibroblast during wound healing. *Journal of Stem Cells & Regenerative Medicine*, **16**(2), 73-79 (2020).

33. Zhao, B., Zhang, X., Han, W., Cheng, J. and Qin, Y. "Wound healing effect of an Astragalus membranaceus polysaccharide and its mechanism," *Molecular Medicine Reports*, **15**, 4077–4083(2017).

34. Nazzal, M., Osman, M., Albeshri, H., Abbas, D. and Angel, C. Wound Healing: Schwartz's Principles of Surgery, 11th ed.; McGraw-Hill Education, *Medical Pub. Division*: New York, NY, USA, (2019).

35. Nam, G., Rangasamy, S., Purushothaman, B. and Song, J.M. The application of bactericidal silver nanoparticles in wound treatment. *Nanomater. Nanotechnol.,* **5**, 23 (2015).

36. Alhajj, M. and Goyal, A. Physiology, Granulation Tissue.. In: StatPearls [Internet]. Treasure Island (FL): StatPearls Publishing; Jan-. Available from: https://www.ncbi.nlm.nih.gov/books/NBK554402/(2023).

37. Xiao, T., Yan, Z., Xiao, S. and Xia, Y. Proinflammatory cytokines regulate epidermal stem cells in wound epithelialization. *Stem Cell Research & Therapy*, **11** (1), 232 (2020).

38. You, C., Li, Q., Wang, X., Wu, P.,Ho, J.K., Jin, R., Zhang, L., Shao, H. and Han, C. Silver nanoparticle loaded collagen/chitosan scaffolds promote wound healing via regulating fibroblast migration and macrophage activation. *Scientific. Reports*, **7**, 10489 (2017).

39. Baygar, T., Sarac, N., Ugur, A. and Karaca, I.R. Antimicrobial characteristics and biocompatibility of the surgical sutures coated with biosynthesized silver nanoparticles. *Bioorganic Chemistry*, **86**, 254–258 (2018).

40. Raghunath, A. and Perumal, E. Metal oxide nanoparticles as antimicrobial agents: A promise for the future. *International Journal of Antimicrobial. Agents*, **49**, 137–152 (2017).

41. Pormohammad, A. and Turner, R.J. Silver Antibacterial Synergism Activities with Eight Other Metal(loid)-Based Antimicrobials against Escherichia coli, Pseudomonas aeruginosa, and Staphylococcus aureus. *Antibiotics*, **9**, 853 (2020).

42. Bowden, L.G., Byrne, H.M., Maini, P.K. and Moulton, D.E. A morphoelastic model for dermal wound closure. *Biomech Model Mechanobiol*., **15**(3), 663-681 (2016).

43. Fawzy, H., El Shawarby, A., Kalleny, N. and Shaker, S. Comparative Study on the Effect of Silver Nanoparticles versus Silver Sulfadiazine in Diabetic Wound Healing in Albino Rat: a Histological Study. *The Egyptian Journal of Hospital Medicine*, **73** (2), 6042-6051 (2018).

44. Abdal Dayem, A., Hossain, M.K., Lee, S.B., Kim, K., Saha, S.K.,Yang, G.-M., Choi, H.Y. and Cho, S.-G. The Role of Reactive Oxygen Species (ROS) in the Biological Activities of Metallic Nanoparticles. *International Journal of Molecular Science*, **18**, 120 (2017).

45. Talarska, P., Boruczkowski, M. and Żurawski, J. Current Knowledge of Silver and Gold Nanoparticles in Laboratory Research-Application, Toxicity, Cellular Uptake. *Nanomaterials (Basel)*, **11** (9) , 2454 (2021).

46. Khater, H.F., El-Shorbagy, M.M. and Seddiek, S.A. Lousicidal efficacy of camphor oil, d-phenthroin, and deltamethrin against the slender pigeon louse, *Colubicola columbae*. *International Journal of Veterinary Science and Medicine*, **2**, 7-13 (2014).

دور جل مركب الذهب والفضة النانوي مقابل سكريات الاستراغالوس في عملية التئام الجروح المحدثة تجريبيا في الجرذان البيضاء دراسة دوائية ونسيجية مقارنة

فادي سيد يوسف[1]؛ هبة محمد فوزي[2]؛ سامح حامد إسماعيل[3]؛ جهاد جنيدي محمد[4,5]

[1] قسم الأدوية- كلية الطب البيطري- جامعة القاهرة- 12211 الجيزة- مصر.
[2] قسم الأنسجة وبيولوجيا الخلية- كلية الطب جامعة - عين شمس- مصر.
[3] تكنولوجيا النانو للدراسات العليا - جامعة القاهرة - فرع الشيخ زايد الحرم الجامعي، مدينة الشيخ زايد، الجيزة، ص.ب 12588، مصر.
[4] قسم الكيمياء، كلية العلوم- جامعة القاهرة- 12613- الجيزة- مصر.
[5] قسم علوم النانو- معهد العلوم الأساسية والتطبيقية- الجامعة المصرية اليابانية للعلوم والتكنولوجيا- برج العرب الجديدة- الإسكندرية- 21934- مصر.

الهدف من هذا العمل هو تصنيع نوعين للجسيمات النانوية الطبيعية (استراغالوس عديد السكاريد) والمعدنية (الجسيمات النانوية الذهبية والفضية). حيث تمثل طرقا سريعة وبسيطة وغير مكلفة لتحسين قدرة الجسيمات على تعزيز التئام الجروح. تميزت المواد الهلامية النانوية باستخدام المجهر الإلكتروني النافذ ، وإمكانات زيتا ، وتشتت الضوء الديناميكي. تم عرض الشكل الكروي إلى شبه الكروي للهلام النانوي الذهبي الفضي بدون أي تجميع ومع تشتت متجانس في مصفوفة الهلام في صور المجهر الإلكتروني. نظرا للطلاء الفعال لمصفوفة الهلام على المركب النانوي ، وأظهر تشتت الضوء الديناميكي أن الحجم كان 85 نانومتر و (30-50 نانومتر) لجيل المركب النانوي الذهبي والفضي وجيل الاستراغالوس متعدد السكاريد النانوي على التوالي. تم إثبات النشاط الحيوي الممتاز لهلام مركب الذهب والفضة النانوي وهلام Astragalus polysaccharides النانوي من خلال قيم زيتا المحتملة لكل منهما والتي تبلغ -25.2±0.71 مللي فولت و+30.4±1.65 مللي فولت. تم تقييم قدرة هلام المركب النانوي الناتج على إصلاح الجروح في الجسم الحي من خلال التأكيد النسيجي والصور المجهرية التي أظهرت عملية الشفاء. بالمقارنة مع جل مركب الذهب والفضة النانوي ومجموعة التحكم غير المعالجة، أظهرت التحقيقات الدوائية لحجم الجرح والفحوصات التشريحية المرضية للمجموعة المعالجة بعديد السكاريد Astragalus قدرًا أكبر بكثير من إعادة تكوين النسيج الظهاري، وتجديد بصيلات الشعر وα-SMA الطبيعي تقريبًا. يتمتع هلام النانو متعدد السكاريد Astragalus بقدرة أفضل على التئام الجروح بالمقارنة مع هلام المركب النانوي الذهبي والفضي والمجموعات غير المعالجة، وفقًا لنتائجنا للمعاملات الدوائية التي تم فحصها من خلال زيادة إغلاق الجرح في اليوم الخامس عشر مقارنة بالمجموعات الأخرى.

الكلمات الدالة: الذهب - جل مركب نانوي فضي، جل نانو متعدد السكاريد استراغالوس، التئام الجروح، TEM، تشتيت الضوء الديناميكي، التشريح المرضي، الدوائي.